Mechanical compression induces chondrocyte hypertrophy by regulating Runx2 O-GlcNAcylation during temporomandibular joint condyle degeneration

From The Affiliated Hospital of Qingdao University, Qingdao, China

Y. Xiao,[1,2,3] Z. Yue,[4] H. Zijing,[1,3] Z. Yao,[1,2,3] M. Sui,[5] Z. Xuemin,[1,2,3] Z. Qiang,[1,2,3] Y. Xiao,[1,2,3] R. Dapeng[1,2,3]

[1]Department of Orthodontics, The Affiliated Hospital of Qingdao University, Qingdao, China
[2]School of Stomatology, Qingdao University, Qingdao, China
[3]Department of Central Laboratory, The Affiliated Hospital of Qingdao University, Qingdao, China
[4]Department of Orthodontics, Qingdao Municipal Hospital, University of Health and Rehabilitation Sciences, Qingdao, China
[5]College of Materials Science and Engineering, Qingdao University, Qingdao, China

Correspondence should be sent to Ren Dapeng
rendapeng@qdu.edu.cn

Aims
Excessive chondrocyte hypertrophy is a common feature in cartilage degeneration which is susceptible to joint overloading, but the relationship between mechanical overloading and chondrocyte hypertrophy still remains elusive. The aim of our study was to explore the mechanism of mechanical compression-induced chondrocyte hypertrophy.

Methods
In this study, the temporomandibular joint (TMJ) degeneration model was built through forced mandibular retrusion (FMR)-induced compression in TMJ. Chondrocytes were also mechanically compressed in vitro. The role of O-GlcNAcylation in mechanical compression-induced chondrocyte hypertrophy manifested through specific activator Thiamet G and inhibitor OSMI-1.

Results
Both in vivo and in vitro data revealed that chondrocyte hypertrophic differentiation is promoted by compression. Immunofluorescent and immunoblotting results showed that protein pan-O-GlcNAcylation levels were elevated in these hypertrophic chondrocytes. Pharmacologically inhibiting protein pan-O-GlcNAcylation by OSMI-1 partially mitigated the compression-induced hypertrophic differentiation of chondrocytes. Specifically, runt-related transcription factor 2 (Runx2) and SRY-Box 9 transcription factor (Sox9) were subjected to modification of O-GlcNAcylation under mechanical compression, and pharmacological activation or inhibition of O-GlcNAcylation affected the transcriptional activity of Runx2 but not Sox9. Furthermore, compression-induced protein pan-O-GlcNAcylation in chondrocytes was induced by enhanced expression of glucose transporter 1 (GLUT1), and depletion of GLUT1 by WZB117 dampened the effect of compression on chondrocyte hypertrophy.

Conclusion
Our study proposes a novel function of GLUT1-mediated protein O-GlcNAcylation in driving compression-induced hypertrophic differentiation of chondrocytes by O-GlcNAc modification of Runx2, which promoted its transcriptional activity and strengthened the expressions of downstream hypertrophic marker.

Bone & Joint Research

Article focus

- This study investigated the role of O-GlcNAc modification of runt-related transcription factor 2 (Runx2) in promoting hypertrophic differentiation of chondrocytes under mechanical compression.

Key messages

- Both in vivo and in vitro data demonstrated that compression-induced chondrocyte hypertrophy was associated with protein O-GlcNAcylation, and inhibition of O-GlcNAcylation mitigated the chondrocyte hypertrophy under compression.
- O-GlcNAc modification of Runx2 protein resulted in elevated transcriptional activity of Runx2, which accounted for the increased expressions of hypertrophic genes in chondrocytes.
- The increased protein O-GlcNAcylation in chondrocytes under mechanical compression was partially explained by enhanced expression of glucose transporter 1 (GLUT1).

Strengths and limitations

- These data provide a potential mechanism underlying the mechanical overloading-induced chondrocyte hypertrophy and further cartilage degeneration.
- In vitro experiments performed Runx2 silencing in chondrocytes and validated its effect in compression-induced chondrocyte hypertrophy. However, the effect of Runx2 overexpression was not investigated.
- Further transgenic animal and clinical studies are warranted to better elucidate the pathogenesis of cartilage degeneration.

Introduction

Temporomandibular joint (TMJ) degeneration is a progressive degenerative disease that results in cartilage degradation and joint friction, eventually leading to osteoarthritis (OA). Multiple factors, such as systemic factors (ageing, genetic, hormone, immunity) or local factors (trauma, occlusion, anatomy), are related to initiation of TMJ degeneration.[1] Notably, abnormal mechanical loading inside TMJ is a critical element triggering the disruption of TMJ homeostasis, gradually leading to TMJ degeneration.

As the only resident cell type in cartilage, chondrocytes are solely responsible for the homeostatic synthesis of cartilage matrix, the disruption of which contributes to cartilage degeneration. Chondrocyte hypertrophy is a natural phenomenon that usually occurs during endochondral osteogenesis. Hypertrophic chondrocytes, characterized by enlarged cell size and volume, undergo metabolic changes with higher expressions of collagen type X (COL X), runt-related transcription factor 2 (RUNX2), matrix metalloproteinase 13 (MMP13), and alkaline phosphatase (ALP), whereas cartilage matrix proteins such as aggrecan, collagen type II (COL II), and SRY-Box 9 transcription factor (SOX9) are decreased. Abnormal chondrocyte hypertrophy is an important pathological feature in degenerated cartilage, and also plays a vital role in accelerating cartilage degeneration.[2,3] The regulation of chondrocyte hypertrophy has been intensively studied. Signalling pathways, such as Indian hedgehog (Ihh), calcium/calmodulin-dependent

protein kinase II (CaMKII), and parathyroid hormone receptor (PTH1R), were reported to be involved in this process.[1,3] However, how excessive mechanical stimuli could affect chondrocyte hypertrophy has not yet been explored.

O-linked N-acetylglucosaminylation (O-GlcNAcylation) is a post-translational modification of proteins, which is modified by the O-GlcNAc transferase (OGT) and the neutral N-acetylglucosaminidase O-GlcNAcase (OGA). Alterations in protein O-GlcNAcylation have pathogenic roles in various chronic diseases such as diabetes mellitus, cardiovascular disease, neurodegeneration, and cancer.[4] Extracellular glucose concentration is the main factor in regulating intracellular protein O-GlcNAcylation, while other conditions such as oxidative stress, hypoxia, or heat shock have also been reported to orchestrate protein O-GlcNAcylation.[5] Induction of protein O-GlcNAcylation by OGT has been found to promote chondrocyte hypertrophy both in vitro and in vivo.[6] In addition, Frank et al[7] demonstrated for the first time that mechanical compression was able to induce protein O-GlcNAc in human periodontal ligament cells, which was attributed to dynamic cytoskeleton adaption to mechanical stimuli. Based on these studies, we hypothesized that abnormal mechanical loading might cause chondrocyte hypertrophy and TMJ degeneration through dysregulating protein O-GlcNAcylation in chondrocytes.

Methods

Materials and reagents

Alpha-modified Eagle's minimal essential medium (α-MEM), Dulbecco's modified Eagle's medium (DMEM), and fetal bovine serum (FBS) were purchased from Invitrogen (Thermo Fisher Scientific, USA). Antibodies against Runx2 (PA5-86506), Col X (14-9771-82), Col II (PA5-99159), Sox9 (14-9765-82), RL2 (MA1-072), and GLUT1(MA5-31960) were purchased from Thermo Fisher Scientific. Antibodies against ALP (ab229126) and aggrecan (ab313636) were purchased from Abcam (UK), and antibody against glyceraldehyde-3-phosphate dehydrogenase (GAPDH) was purchased from Beyotime (China). All the other chemicals used in this study are described in the subsequent sections.

Animal model establishment

Six-week-old Sprague-Dawley (SD) male rats were used for the following experiments. We adhered to the ARRIVE guidelines and included the ARRIVE checklist as Supplementary Material. SD rats were housed under room temperature (25°C), and randomized into the control group (CON) and experimental groups (EXP). After anaesthesia, rats in the EXP groups were subjected to forced mandibular retrusion (FMR), and were euthanized at two and four weeks. The CON group was euthanized at the same time. During the experiment, both the EXT and CON rats were fed with a liquid diet. For the intra-articular injection of OSMI-1 or WZB117, rats were randomized into three groups (CON, four-week EXP with injection of saline, and four-week EXP with injection of OSMI-1 or WZB117). The condyles of both sides of TMJ were collected for further analysis. For the sample size determination, PASS.15 software (NCSS Statistical Software, USA) was used by inputting the following parameters: type I error (α) was set as 0.05, type I error (β) was set as 0.1, and the means and SDs of each group were calculated in GraphPad Prism 9 software (GraphPad

Software, USA) based on our pilot experiments. The sample size was calculated using PASS.15 software as follows:

$$N = \frac{\lambda}{\Delta}; \ \Delta \frac{1}{\sigma^2} \sum_{i=1}^{k} (\mu_i - \overline{\mu})^2; \ \overline{\mu} = \frac{1}{k} \sum_{j=1}^{k} \mu_j; \ \lambda = N \frac{\sigma_m^2}{\sigma^2}$$

Where N is the sample size, σ is the SD, k is the group number, and μ_i is the mean of each group. λ does not need to be inputted in PASS.15 software.

H&E and Safranin O/Fast Green staining

The mandibular condyles of rats were dissected and fixed with 4% paraformaldehyde, decalcified with 4% ethylenediamine-tetraacetic acid (EDTA) for four weeks, dehydrated in ethanol, embedded in paraffin, and sagittally cut into 5 µm-thick serial sections. The central sagittal sections of each condyle were selected randomly for haematoxylin and eosin (H&E) staining and Safranin O/Fast Green staining. The H&E staining kit (C0105S) was purchased from Beyotime, and Safranin O/Fast Green staining kit (S0335) was purchased from Bioss Antibodies (USA).

For the quantification of proliferative zone height and hypertrophic zone height, three condyle sections in each rat were randomly selected, and each condyle section was delineated the top of the proliferative zone, the junction between the proliferative zone and the hypertrophic zone, and the chondro-osseous junction. These zones were established based on the morphological characteristics of the chondro-cytes, and on the changes in matrix staining. The vertical height of each zone was measured at similar intervals across the sections (n = 5 per section). Values for each individual rat were obtained by averaging all 30 measurements (3 sections × 5 locations × 2 (left and right sides)) per animal. For hypertro-phic chondrocyte size determination, three locations (30 µm × 40 µm) were randomly selected in the hypertrophic zone in each section, and values for each individual rat were obtained by averaging all measurements (3 sections × 3 locations × n cell numbers in each location × 2 (left and right sides)) per animal.

Safranin O/Fast Green staining was used to visual-ize proteoglycans in the articular cartilage. The severity of degeneration was evaluated in the TMJ condyle with at least five sections of Safranin O/Fast Green staining using the Osteoarthritis Research Society International (OARSI)[8] scoring system by four observers blinded to group-identifying information.

Micro-CT scanning

After two and four weeks, the condyles of rats were dissec-ted and fixed in 4% paraformaldehyde for micro-CT scanning (PerkinElmer Quantum GX2, USA). The scan condition was set at 70 kV, the electrical flow was 60 µA, the exposure time was set at 4,000 ms, and the resolution was set at 12 µm. 3D images of the micro-CT slices were used for comparison and evaluation of subchondral bone resorption. Calculations of the relevant microstructural parameters, including bone mineral density (BMD), bone volume fraction (BV/TV), bone trabecular number (Tb.N), trabecular thickness (Tb.Th), and trabecular space (Tb.Sp), were analyzed using Simple Viewer (DeBrosse Consulting, UK).

IHC and IF staining

The sections for IHC and IF staining were prepared similar to those for H&E staining. For IHC staining, the sections were incubated with the primary antibody against Sox9, Runx2, Col X, and RL2 overnight at 4℃. Following this, sections were incubated with horseradish peroxidase (HRP)-conjugated goat antirabbit immunoglobulin G (IgG) polyclonal antibody at 37℃ for one hour. The signal developed as a brown reaction product using the peroxidase substrate 3,3-diaminobenzidine (Bioss Bioscience, China). For quantification of Sox9, Runx2, Col X, and RL2 positive cell percentage in IHC staining, the region of interest (ROI) fields (50 µm × 40 µm) were ran-domly chosen in each sample. For IF staining, the sections were incubated with primary antibody against RL2 and Col X, and mixed at appropriate ratios before incubation overnight at 4℃. DAPI staining was performed after incubation with fluorescent-labelled secondary antibodies. Digital images were obtained using a laser scanning confocal microscope (Nikon, Japan). For IF staining of in vitro compressed chondrocytes, cells were first cultured on 0.1% Gelatin (Sigma-Aldrich, USA) pre-coated glass coverslips. After mechanical compression experiments, culturing medium was removed, and the cells were fixed with 4% formaldehyde containing 0.1% glutaralde-hyde for 15 minutes at 37℃. After being rinsed with cold PBS (pH 7.4), the cells were permeabilized using 0.1% Triton X-100 (Fisher) for ten minutes, and then incubated with 1% bovine serum albumin for one hour at room temperature. Antibodies against Sox9, Runx2, and RL2 were added, and the fixed cells were incubated with antibodies at 4℃ overnight followed by incubation with anti-IgG-fluorescein isothiocyanate (FITC) and IgG-Texas Red (1:150 dilution) for one hour. After removal of antibodies, cells were rinsed with PBS and mounted with 90% glycerol. DAPI staining was conducted right after washing with PBS. Fluorescence was immediately observed using a Nikon ECLIPSE E400 microscope.

Intra-articular administration of OSMI-1 or WZB117

To pharmacologically inhibit O-GlcNAcylation or block GLUT1 expression in rat TMJ cartilage, OSMI-1 (Sigma, SML1621) or WZB117 (Sigma, SML0621), respectively, were injected intra-articularly. Briefly, OSMI-1 was dissolved in dimethyl sulfoxide (DMSO) in a final concentration of 10 mg/ml, and the OSMI-1 solution was injected directly via intra-articular manner into both sides of rat TMJ (0.5 ml for one side). Similarly, WZB117 was dissolved in DMSO in a final concen-tration of 10 mg/ml, and the WZB117 solution was injected directly intra-articularly into both sides of rat TMJ (1 ml for one side). The intra-articular injection process was repeated each day for the duration of the experiment, whereas control animals were injected with DMSO. After that, animals of both control and experimental groups were killed and TMJ samples were prepared for H&E staining, Safranin O/Fast Green staining, immunohistochemistry, and immunofluores-cence staining.

Primary culture and mechanical compression of TMJ condyle chondrocytes

Rat TMJ cartilage tissues were scraped from the condyle surface, and were treated with 0.5% type II collagenase for four hours at 37℃. Isolated chondrocytes were centrifuged and resuspended with α-MEM. The synovial macrophages

Mechanical compression induces chondrocyte hypertrophy by regulating Runx2 O-GlcNAcylation during TMJ condyle degeneration
Y. Xiao, Z. Yue, H. Zijing, et al

211

were maintained in culture for one week in α-MEM containing 15% FBS and 100 ng/ml macrophage colony-stimulating factor, while the condyle chondrocytes were cultured in α-MEM containing 15% FBS. After two to three passages, the chondrocytes were incubated in a commercial mechanical compression stimulator (NK-P40; Naturethink, China), and subjected to a cyclic compression protocol (50, 100, 200, 300, and 400 kPa; 0.1 Hz) for three days. For inhibition of O-GlcNAcylation, OSMI-1 was added into culture medium in a final concentration of 20 μM during mechanical compression; for inhibition of GLUT1, WZB117 was added into culture medium in a final concentration of 40 μM during mechanical compression. After three days' mechanical compression, cells were collected for the following experiments.

qRT-PCR

Total messenger RNA (mRNA) was extracted from compressed chondrocytes using an RNA purification kit (Corning, USA) according to the manufacturer's instructions. Reverse transcription (RT) was performed using the PrimeScript RT Reagent Kit (TaKaRa, Japan). Real-time polymerase chain reaction (PCR) was carried out using SYBR Premix Ex Taq (Perfect Real Time, Takara). Then, quantitative PCR was performed using LightCycler 96 System (Roche, Switzerland) with the following primers: *gapdh*, forward 5'-AAAGGGTCATCATCTCTG-3', reverse 5'-GCTGTTGTCATACTTCTC-3'; *col II*, forward 5'-GACCTGCCGGTGAACAAG-3', reverse 5'-GGTACCAGGTTCTCCATCTCT-3'; *col X*, forward 5'-GATCATGGAGCTCACGGAAAA-3', reverse 5'-CCGTTCGATTCCGCATTG-3'; *runx2*, forward 5'-TCTTCCCAAAGCCAGAGCG-3', reverse 5'-TGCCATTCGAGGTGGTCG-3'; *sox9*, forward 5'-CTCTCCTAACGCCATCTTCAAG-3', reverse 5'-ACGTCTGTTTT GGGAGTGG-3'; *alp*, forward 5'-CCCGAGTGCTTTGTGTGTGCTG-3', reverse 5'- CCGCCGGTGTTCGTGTGTG-3'; *aggrecan*, forward 5'-GCAGACATTGATGAGTGCCTC-3', reverse 5'-CTCACACAGGTCCCCTCTGT-3'; *glut1*, forward 5'-ATGATGCGGGAGAAGAAGGT-3', reverse 5'-GAACAGCGACACCACAGTGA-3'. The results were presented as the calculated comparative expression ratios of the target sample to control group for each sample using the CT method ($2^{-\Delta\Delta CT}$).

Co-immunoprecipitation and immunoblotting

After compression, the cells were washed three times with ice-cold phosphate-buffered saline (PBS) and solubilized in lysis buffer. The lysates were then centrifuged for 15 minutes at 4°C at 16,000 ×g and with Runx2 or Sox9 antibodies for 16 hours at 4°C, followed by immunoprecipitation with protein G-agarose (Santa Cruz Biotechnology, USA). Immunoprecipitates were washed five times with lysis buffer, boiled in sodium dodecyl sulfate (SDS) sample buffer, collected using magnets, and heated at 95°C for two minutes. Finally, the immunoprecipitates were subjected to SDS-polyacrylamide gel electrophoresis (PAGE) and immunoblot analysis as described in the following section.

The compressed chondrocytes were washed with PBS precooled at 4°C and lysed using radioimmunoprecipitation assay (RIPA) buffer. The cell lysate was centrifuged and the supernatant was separated at 14,000 ×g and 4°C for ten minutes. Proteins were measured using the bicinchoninic acid (BCA) protein assay. SDS-PAGE electrophoresis, transferring, fixation, incubation, and development were performed. The concentrations of primary antibodies for RL2, Sox9, Col II, Aggrecan, Runx2, Col X, ALP, and Glut1 were 1:1,000. Finally, the expressions of the specific proteins were quantified.

Luciferase reporter gene assay

Before applying external mechanical strain, chondrocytes were cultured until 70% to 80% confluence, and were transfected with luciferase reporter plasmids constructed in the pGL2 basic vector: p-4Col2a1-luc harboring four murine Col2a1 promoter and p-6OSE2-luc harboring six murine OSE2 promoter. The pMSVβ-gal plasmid was constructed in the pGL2 basic vector, in which luciferase activity for each promoter construct could be normalized for transfection efficiency in all experiments. For transient transfections, cells in each well were incubated in 1 ml of serum-free medium containing 6 μg of Lipofectamine, 0.4 μg of p-4Col2a1-luc or p-6OSE2-luc, and 0.4 μg of the pMSVβ-gal expression plasmid. Transfection was terminated after 12 hours by replacing transfection medium with serum-free DMEM. Cells were then incubated in serum-free medium for an additional 48 hours with or without being subjected to mechanical compression. To measure the contribution of O-GlcNAcylation to compression-induced effects on promoter activity, pharmacological inhibitor OSMI-1 and activator Thiamet G were included in the medium of control or compressed cells after transient transfection. DMSO was used as a negative control. To measure luciferase activity, cell lysates were collected and assayed using the Luciferase Assay System (Promega, USA) as per the manufacturer's instructions. Cells were washed with ice-cold Hanks' balanced salt solution, then scraped off of each well using cell lysis buffer. Afterward the cell lysate was centrifuged, and luciferase activity was measured in the supernatant using a Berthold Lumat LB 9507 Luminometer (Berthold Technologies, Germany). Luciferase activity was normalized to relative β-galactosidase activity.

Statistical analysis

Statistical analysis was performed using GraphPad Prism 6.0 (GraphPad Software) and SPSS 11.0 software (SPSS, USA). One-way analysis of variance (ANOVA) was used for multiple comparisons among the groups. The independent-samples *t*-test was used between compared groups. All data are presented as the mean and SD. A p-value of < 0.05 was considered statistically significant.

Results
FMR resulted in TMJ degeneration

First, we investigated whether long-term mandibular retrusion could lead to TMJ degeneration. The FMR animal models were built and confirmed by radiograph (Figure 1a and Figure 2). TMJ samples were collected two weeks and four weeks after FMR. Safranin O/Fast Green staining demonstrated that TMJ cartilage degradation was apparent following FMR, revealed by lower glycosaminoglycan content compared with the control group (Figures 3b and 3c). In addition, micro-CT results displayed obvious condyle subchondral bone resorption in two-week and four-week FMR groups (Figures 3d to 3i). Thus, mandibular retrusion is a potential pathogenic factor leading to TMJ degeneration.
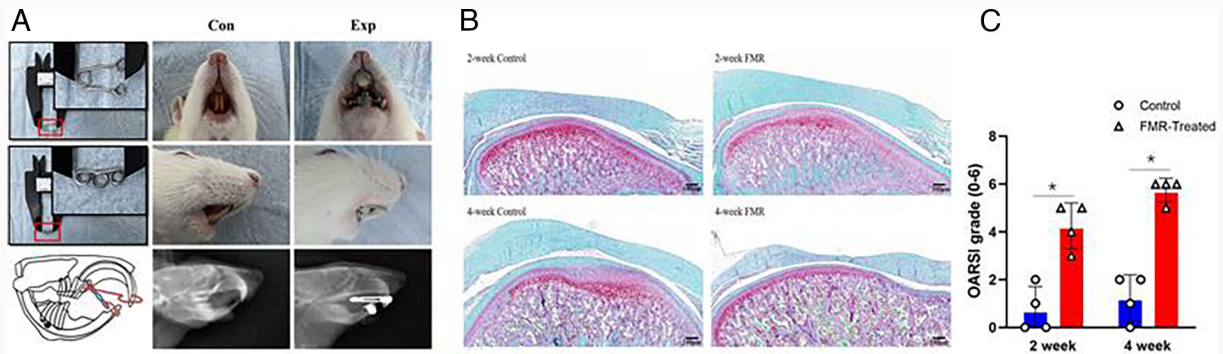
Fig. 1
Forced mandibular retrusion (FMR) resulted in temporomandibular joint (TMJ) degeneration. a) Upper and lower jaw gears made of stainless steel; diagram of FMR animal model; frontal view of animal in control group; lateral view of animal in control group; jaw radiograph of animal in control group; frontal view of animal in FMR group; lateral view of animal in FMR group; and jaw radiograph of animal in FMR group. b) Safranin O/Fast Green staining of mandibular condyles in control and experimental groups at two and four weeks. Scale bar: 100 μm. c) Graph showing the Osteoarthritis Research Society International (OARSI) score in two- and four-week FMR groups (n = 2 rat/group). *p < 0.05, **p < 0.01, independent-samples *t*-test.
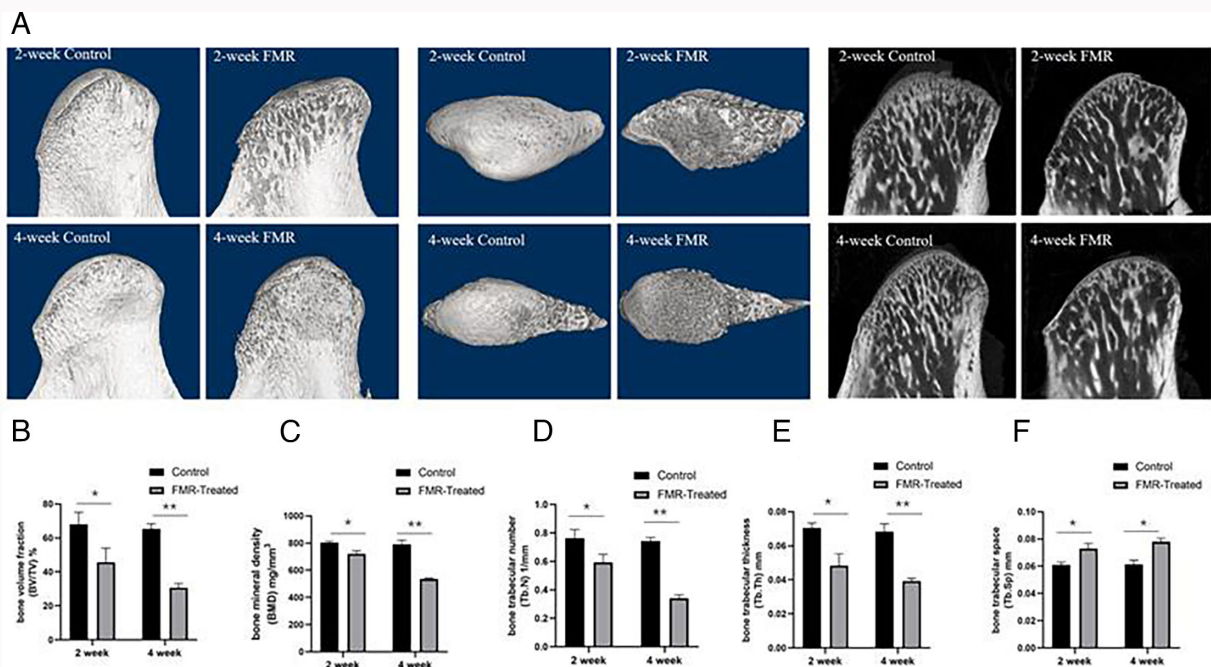

Fig. 2
a) Representative 3D and 2D micro-CT samples from two- and four-week control and experimental groups. b) Bone volume fraction (BV/TV) analysis. c) Bone mineral density (BMD) analysis. d) Bone trabecular number (Tb.N) analysis. e) Bone trabecular thickness (Tb.Th) analysis. f) Bone trabecular space (Tb.Sp) analysis. These micro-CT parameters were analyzed using one-way analysis of variance to compare data among control group and experimental groups (2 wks and 4 wks), n = 4 rat/group. *p < 0.05, **p < 0.01, *t*-test. FMR, forced mandibular retrusion.

Excessive chondrocyte hypertrophy occurred in FMR-induced TMJ degeneration

In cartilage, chondrocytes undergo hypertrophy in deeper layers adjacent to subchondral bone. However, abnormal hypertrophic differentiation of chondrocytes led to diminished cartilage matrix production and enhanced endochondral ossification, which escalate cartilage degeneration. We first confirmed that the height of hypertrophic layer of cartilage increased, whereas the height of proliferative layer of cartilage decreased, during FMR-induced TMJ degeneration (Figures 3a to 3c). Moreover, the mean size of hypertrophic chondrocytes in FMR groups was also greater than in the control groups (Figures 3a and 3d). The specific hypertrophic markers

Runx2 (Figures 3e and 3f) and Col X (Figures 3g and 3h) were elevated, whereas the chondrogenetic marker Sox9 (Figures 3i and 3j) decreased, in chondrocytes in FMR groups, compared with those in control groups. Altogether, these results highlight the fact that chondrocytes underwent excessively hypertrophic changes in FMR-induced TMJ degeneration.

Intracellular O-GlcNAcylation was involved in regulating chondrocyte hypertrophy in FMR-induced TMJ degeneration

Next, we investigated how pan-O-GlcNAcylation was altered in FMR-induced TMJ degeneration. O-GlcNAcylation immunohistochemical staining of TMJ cartilage revealed that
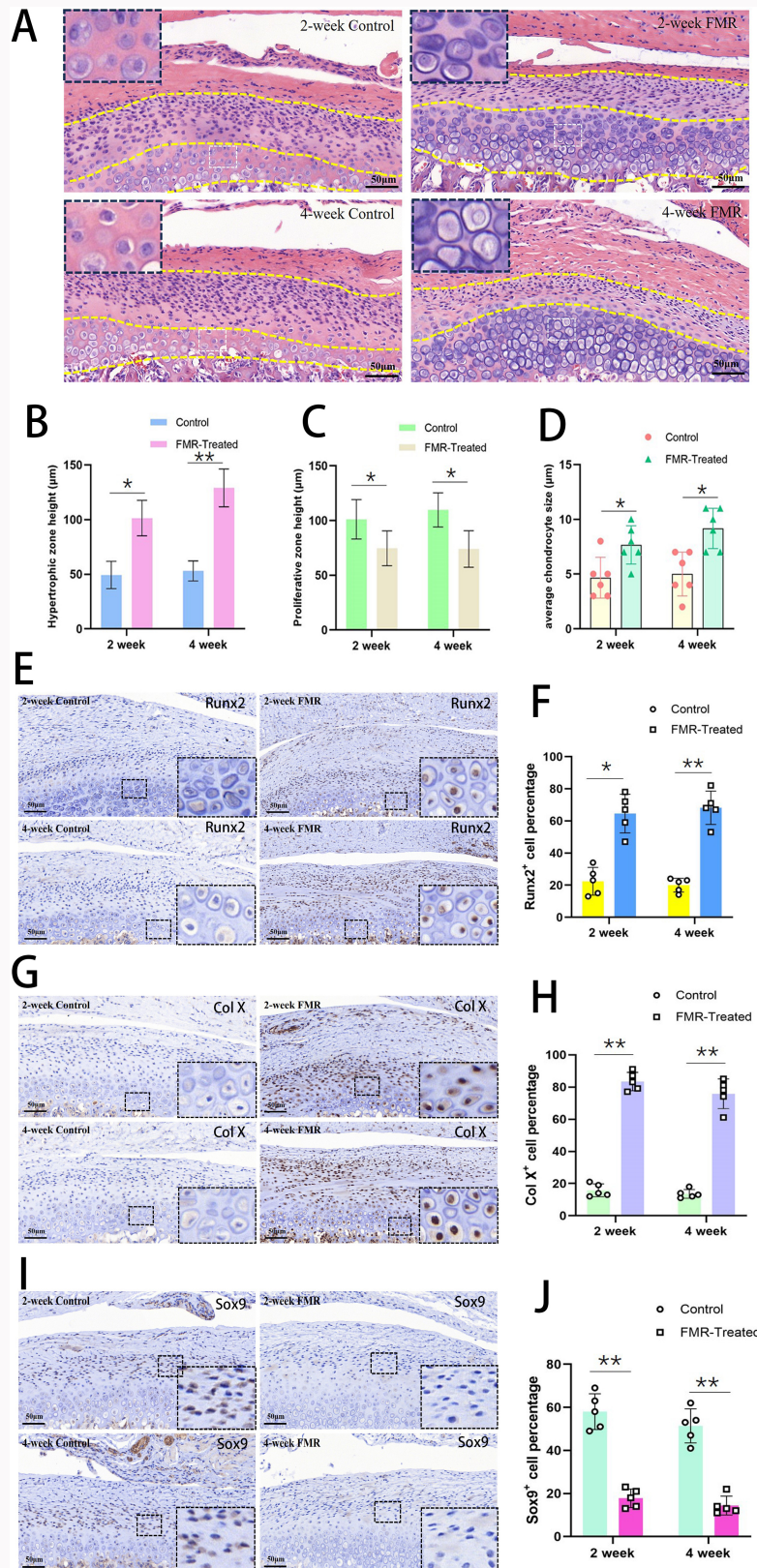
Fig. 3

Excessive chondrocyte hypertrophy occurred in forced mandibular retrusion (FMR)-induced temporomandibular joint (TMJ) degeneration. a) Haematoxylin and eosin (H&E) staining of mandibular condyles in control and experimental groups at two and four weeks. Yellow dashed lines mark the upper proliferative zone and lower hypertrophic zone in cartilage; n = 2 rat/group. Scale bar: 50 μm. b) Graph showing the hypertrophic zone height in control and experimental groups at two and four weeks. c) Graph showing the proliferative zone height in control and experimental groups at two and four weeks. d) Graph showing the average chondrocyte size in control and experimental groups at two and four weeks. e) Representative Runx2 immunohistochemistry staining of condyles in control and experimental groups at two and four weeks. f) Graph showing the Runx2 positive cell percentage according to immunohistochemistry staining of condyles in control and experimental groups at two and four weeks. g) Representative Col X immunohistochemistry staining of condyles in control and experimental groups at two and four weeks. h) Graph showing the Col X positive cell percentage according to immunohistochemistry staining of condyles in control and experimental groups at two and four weeks. i) Representative Sox9 immunohistochemistry staining of condyles in control and experimental groups at two and four weeks. j) Graph showing the Sox9 positive cell percentage according to immunohistochemistry staining of condyles in control and experimental groups at two and four weeks. n = 3 rat/group. *p < 0.05, **p < 0.01, *t*-test. Scale bar: 50 μm.

chondrocytes of full cartilage layer exhibited pan-O-GlcNAcylation under normal conditions (Figure 4a). In response to FMR for two and four weeks, chondrocytes in cartilage displayed significantly higher levels of pan-O-GlcNAcylation compared to the control groups (Figures 4a and 4b). In addition, double immunofluorescence staining of hypertrophic marker Col X and pan-O-GlcNAcylation further confirmed that hypertrophic chondrocytes were the major group of cells in cartilage that underwent increased intracellular pan-O-GlcNAcylation in FMR-induced TMJ degeneration (Figure 4c).

To further clarify the role of O-GlcNAcylation in chondrocyte hypertrophic transition, the rats were intra-articularly injected with OSMI-1, a cell-permeable O-GlcNAc transferase (OGT) inhibitor, to block O-GlcNAcylation in chondrocytes. IHC staining showed that FMR-induced elevated pan-O-GlcNAcylation level in condyle chondrocytes was decreased by OSMI-1 administration (Figures 4d and 4e). The level of hypertrophic marker Col X in TMJ condyle was reduced in FMR group receiving OSMI-1 administration, compared to the rats that received PBS administration (Figures 4f and 4g). However, the level of another hypertrophic marker Runx2 was not significantly changed upon OSMI-1 administration (Figures 4h and 4i). Notably, chondrocyte hypertrophy was also partially blunted by OSMI-1 administration (Figures 4j and 4m). Thus, elevated chondrocyte O-GlcNAcylation level following FMR played a role in promoting chondrocyte hypertrophy.

Mechanical compression-induced chondrocyte hypertrophy partially relied on O-GlcNAcylation of Runx2

A recent 3D finite element study demonstrated that the TMJ condyle suffered from overloaded mechanical compression by FMR.[9] Therefore, we postulated that abnormal mechanical loading increased the likelihood of chondrocyte hypertrophy. To test this hypothesis, isolated chondrocytes were mechanically compressed in vitro for three days. Runx2 is the key transcription factor in triggering hypertrophic change of chondrocytes, while Sox9 is critical in maintaining the chondrogenic phenotype. The mRNA and protein levels of hypertrophic markers (Runx2, Col X, and ALP) were increased under higher magnitudes of compression, whereas those of chondrogenic markers (Sox9, Col II, and Aggrecan) were decreased in these groups (Figures 5a and 5b). Hence, mechanical overloading facilitated the hypertrophic transition of in vitro cultured chondrocytes.

The intracellular pan-O-GlcNAcylation level in chondrocytes was analyzed in chondrocytes under different magnitudes of compression. Since higher magnitude of compression (400 KPa) had the most obvious effect in propelling chondrocyte hypertrophy and intracellular pan-O-GlcNAcylation, we chose this magnitude for the following experiments (Figures 5a and 5b). Double immunofluorescence and co-immunoprecipitation results showed that both Runx2 and Sox9 proteins were O-GlcNAc-modified after mechanical compression, compared to the static condition (Figures 5c and 5d). Moreover, the activity of Runx2 and Sox9 proteins was examined using luciferase reporter gene assays. The activity of Runx2 increased, while that of Sox9 decreased, in mechanically compressed chondrocytes, compared to the control chondrocytes (Figure 5e).

To further verify the potential effect of O-GlcNAcylation on protein levels and activities of Runx2 and Sox9, Thiamet G,

a selective inhibitor of O-GlcNAcase (OGA), and OSMI-1 were separately added into chondrocyte culture medium. In static culturing condition, addition of Thiamet G and OSMI-1 had minor effects on Runx2 and Sox9 expressions and activities (Figure 5f). Interestingly, when chondrocytes were subjected to compression, Thiamet G promoted Runx2 activity, whereas neither Runx2 and Sox9 expression nor Sox9 activity were affected by Thiamet G (Figures 5e and 5f). By contrast, OSMI-1 had the opposite effects on Runx2 activity compared to Thiamet G, but did not affect Runx2 and Sox9 expression or Sox9 activity (Figures 5e and 5f).

The mRNA and protein expressions of downstream targets of Runx2 (Col X and ALP) and Sox9 (Col II and aggrecan) were further examined in compressed chondrocytes with pharmacological intervention. Thiamet G increased the levels of Col X and ALP, whereas OSMI-1 had the opposite effect on expressions of these markers (Figures 5g and 5h). This suggests that increased pan-O-GlcNAcylation by mechanical compression promoted chondrocyte hypertrophy in vitro. To investigate whether Runx2 was involved in this process, chondrocytes were transfected with Runx2 shRNA plasmid. Knockdown of Runx2 prohibited the elevations of Col X and ALP induced by mechanical compression with or without addition of Thiamet G (Figures 5g and 5h). In contrast to Col X and ALP, expressions of Col II and Aggrecan were not affected by Thiamet G or OSMI-1, similar to the results for Sox9 (Figures 5g and 5h). Altogether, these results demonstrate that mechanical compression-induced chondrocyte hypertrophy was rendered by hyper-O-GlcNAcylation of Runx2, leading to increased activity of Runx2 and activation of downstream targets (Col X and ALP). However, the decreased expressions of chondrogenetic markers (Sox9, Col II, and aggrecan) upon mechanical compression were not dependent on O-GlcNAcylation modification.

GLUT1 mediated hyper-O-GlcNAcylation and hypertrophic transition

Since glucose transporter (GLUT)-mediated glucose uptake is necessary for the hexosamine biosynthetic pathway (HBP) and O-GlcNAcylation,[10] it is reasonable to speculate that compressive stress activates O-GlcNAcylation by influencing GLUTs. As an ubiquitously expressed protein, GLUT-1 has been proven to be dysregulated in degenerated chondrocytes.[11] We first confirmed that GLUT-1 expression was elevated in chondrocytes both in our animal model and in mechanically compressed chondrocytes in vitro (Figures 6a to 6c). Moreover, inhibition of GLUT-1 with WZB117 significantly suppressed hyper-O-GlcNAcylation in chondrocytes in vivo and in vitro, compared to vehicle control groups with the addition of DMSO (Figures 6d and 6e). Furthermore, administration of WZB117 also partially blunted chondrocyte hypertrophy, both in the rat model and in mechanically compressed chondrocytes in vitro (Figures 6f to 6k). Therefore, these data are sufficient to clarify that compression-induced GLUT-1 elevation plays a role in promoting chondrocyte hyper-O-GlcNAcylation and hypertrophic transition.

Discussion

Occlusal problems inevitably cause abnormal mechanical environments in TMJ, which are the specific factors leading to TMJ degeneration, in addition to other potential factors
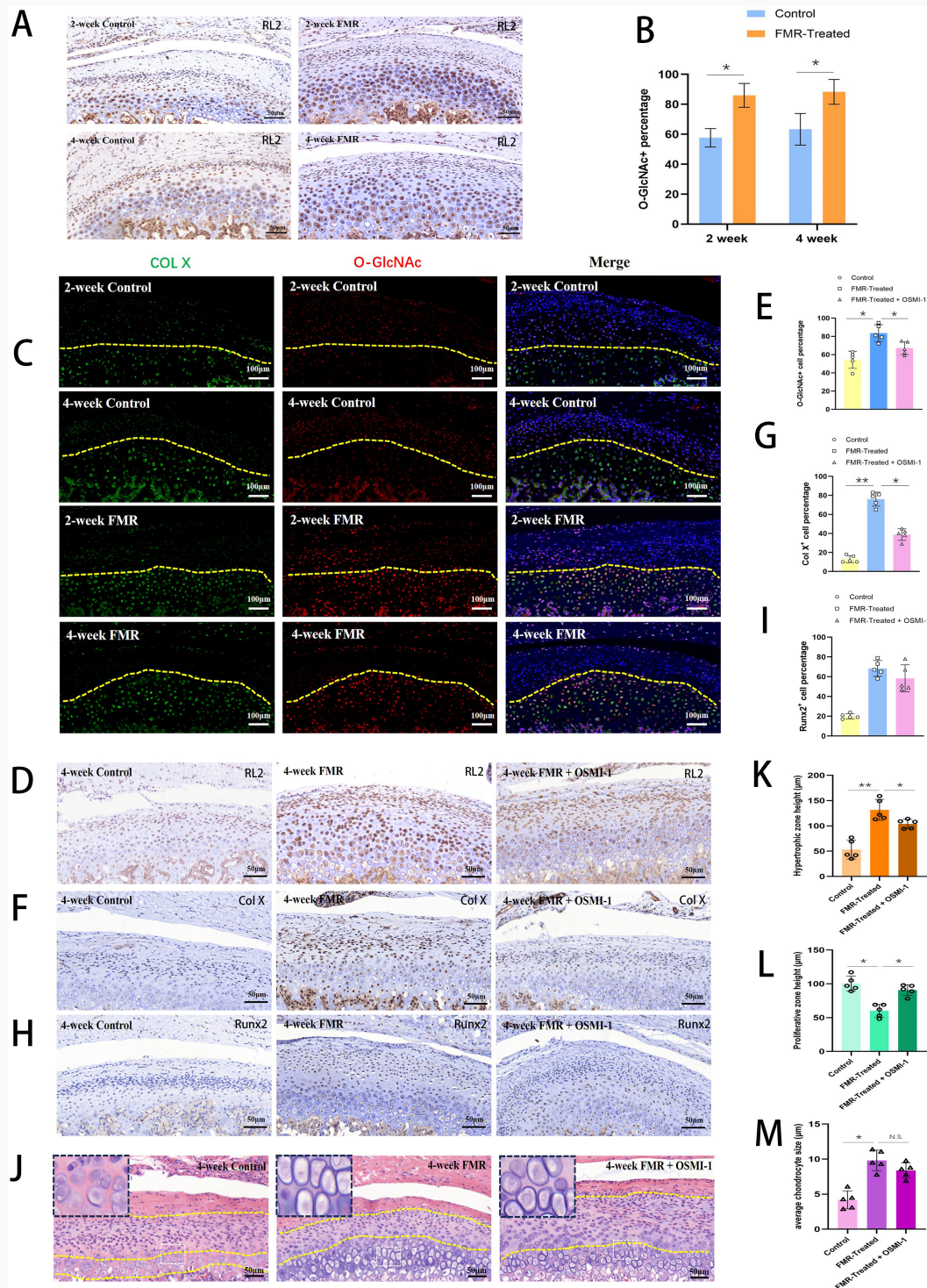
Mechanical compression induces chondrocyte hypertrophy by regulating Runx2 O-GlcNAcylation during TMJ condyle degeneration
Y. Xiao, Z. Yue, H. Zijing, et al

215

Fig. 4

Intracellular O-GlcNAcylation was involved in regulating chondrocyte hypertrophy in forced mandibular retrusion (FMR)-induced temporomandibular joint (TMJ) degeneration. a) Representative RL2 immunohistochemistry staining of condyles in control and experimental groups at two and four weeks. Scale bar: 50 μm. b) Graph showing the O-GlcNAc positive cell percentage according to immunohistochemistry staining of condyles in control and experimental groups at two and four weeks. c) Representative RL2 and Col X double immunofluorescence staining of condyles in control and experimental groups at two and four weeks. Scale bar: 100 μm. d) Representative RL2 immunohistochemistry staining of condyles in four-week control, four-week FMR, and four-week FMR administered with OSMI-1 groups. e) Graph showing the O-GlcNAc positive cell percentage according to immunohistochemistry staining of condyles in four-week control, four-week FMR, and four-week FMR administered with OSMI-1 groups. f) Representative Col X immunohistochemistry staining of condyles in four-week control, four-week FMR, and four-week FMR administered with OSMI-1 groups. g) Graph showing the Col X positive cell percentage according to immunohistochemistry staining of condyles in four-week control, four-week FMR, and four-week FMR administered with OSMI-1 groups. h) Representative Runx2 immunohistochemistry staining of condyles in four-week control, four-week FMR, and four-week FMR administered with OSMI-1 groups. i) Graph showing the Runx2 positive cell percentage according to immunohistochemistry staining of condyles in four-week control, four-week FMR, and four-week FMR administered with OSMI-1 groups. Scale bar: 50 μm. N = 3 rat/group. *p < 0.05, **p < 0.01. j) H&E staining of mandibular condyles in four-week control, four-week FMR, and four-week FMR administered with OSMI-1 groups. Yellow dashed lines mark the upper proliferative zone and lower hypertrophic zone in cartilage. N = 2 rat/group. Scale bar: 50 μm. k) Graph showing the hypertrophic zone height in four-week control, four-week FMR, and four-week FMR administered with OSMI-1 groups. l) Graph showing the proliferative zone height in four-week control, four-week FMR, and four-week FMR administered with OSMI-1 groups. m) Graph showing the average chondrocyte size in four-week control, four-week FMR, and four-week FMR administered with OSMI-1 groups. *p < 0.05, **p < 0.01, one-way analysis of variance. N. S., not significant.
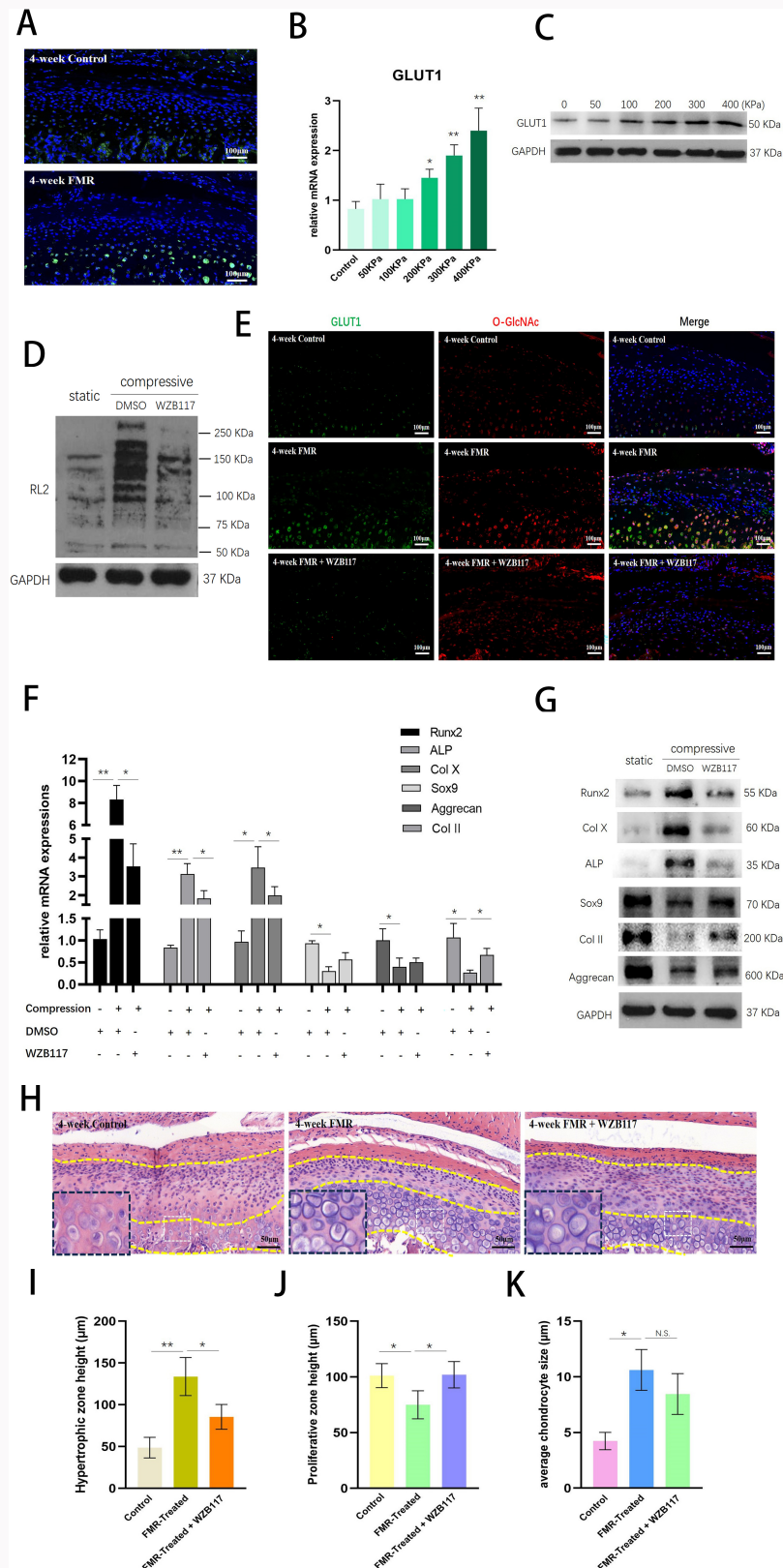
Fig. 5

Mechanical compression-induced chondrocyte hypertrophy partially relied on O-GlcNAcylation of Runx2. a) Quantitative real-time reverse transcription polymerase chain reaction (qRT-PCR) results of *Runx2*, *Sox9*, *Col X*, *Col II*, alkaline phosphatase (*ALP*), and *aggrecan* messenger RNA (mRNA) levels in chondrocytes after mechanical compression at different magnitudes. b) Western blot results of Runx2, Sox9, Col X, Col II, ALP, aggrecan, and O-GlcNAc protein levels in chondrocytes after mechanical compression at different magnitudes. c) RL2 and Sox9 or Runx2 double immunofluorescence staining of chondrocytes after mechanical compression at 400 kPa. Scale bar: 50 μm. d) Co-immunoprecipitation and immunoblotting of Runx2 or Sox9 with RL2 antibody, in chondrocytes after mechanical compression at 400 kPa. e) Western blot results of Runx2, Sox9, and O-GlcNAc protein levels in chondrocytes after mechanical compression at 400 kPa, with the addition of dimethyl sulfoxide (DMSO), Thiamet G, or OSMI-1. f) Luciferase reporter gene assay of Runx2 and Sox9 activities in chondrocytes after mechanical compression at 400 kPa, with addition of DMSO, Thiamet G, or OSMI-1. g) qRT-PCR results of Col X, Col II, ALP, and aggrecan mRNA levels in chondrocytes transfected with Runx2 short hairpin RNA (shRNA) or scrambled shRNA, with the addition of DMSO, Thiamet G, or OSMI-1. h) Western blots results of Col X, Col II, ALP, and aggrecan protein levels in chondrocytes transfected with Runx2 shRNA or scrambled shRNA, with addition of DMSO, Thiamet G, or OSMI-1. *p < 0.05, **p < 0.01. N. S., not significant. GAPDH, glyceraldehyde-3-phosphate dehydrogenase.
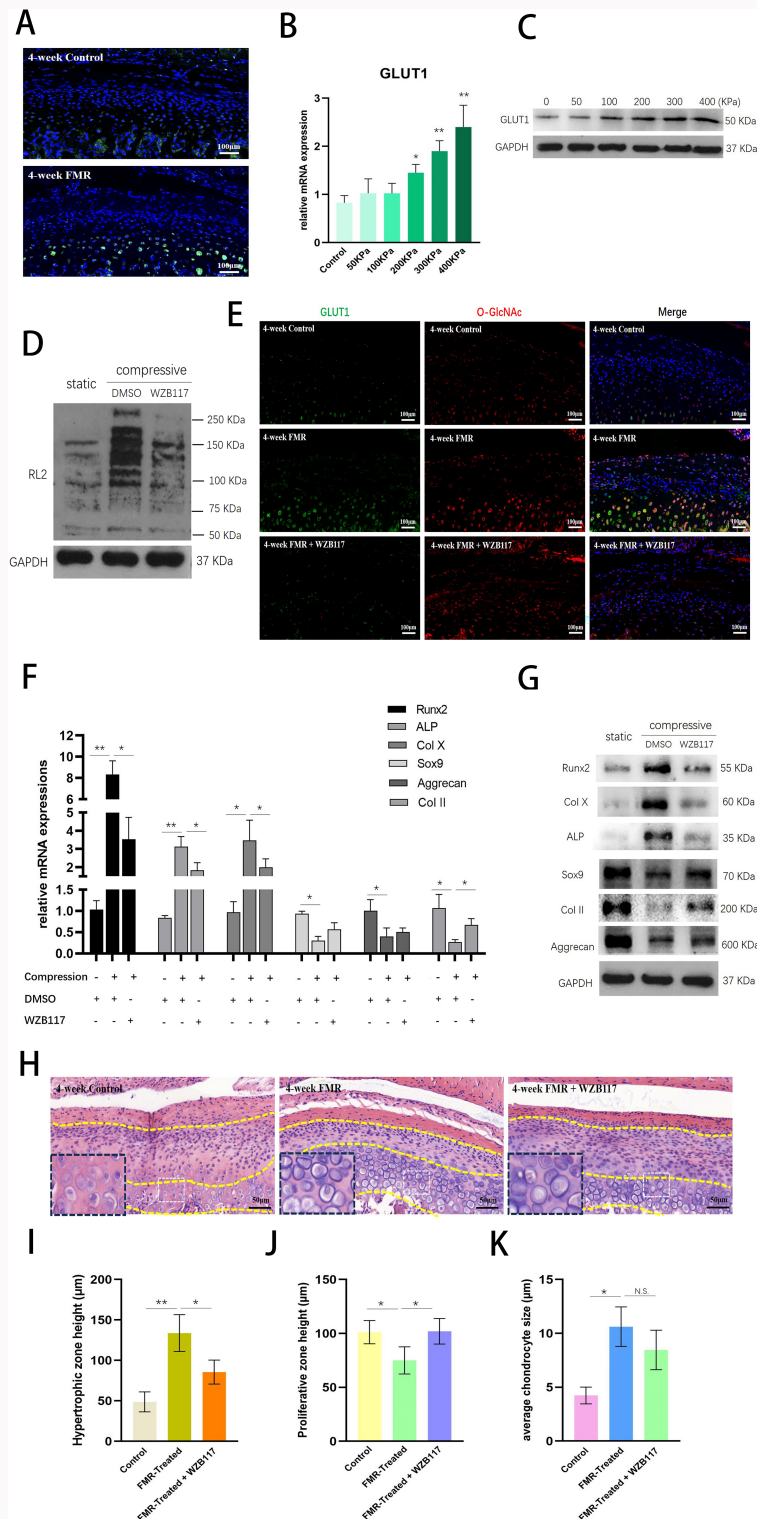
Fig. 6

Glucose transporter (Glut-1) mediated mechanical compression-induced chondrocyte hyper-O-GlcNAcylation and hypertrophic transition. a) Representative Glut-1 immunofluorescence staining of condyles in control and experimental groups at four weeks. N = 2 rat/group. Scale bar: 100 μm. b) Quantitative real-time reverse transcription polymerase chain reaction (qRT-PCR) result of Glut-1 messenger RNA (mRNA) level in chondrocytes after mechanical compression at different magnitudes. c) Western blot result of Glut-1 protein level in chondrocytes after mechanical compression at different magnitudes. d) Western blot result of O-GlcNAc protein levels in chondrocytes after mechanical compression at 400 kPa, with addition of dimethyl sulfoxide (DMSO) or WZB117. e) Representative Glut-1 and RL2 double immunofluorescence staining of condyles in control, four-week forced mandibular retrusion (FMR), and four-week FMR with administration of WZB117 at four weeks. Scale bar: 100 μm. f) qRT-PCR results of Runx2, Sox9, Col X, Col II, alkaline phosphatase (ALP), and aggrecan mRNA levels in chondrocytes after mechanical compression at 400 kPa, with the addition of DMSO or WZB117. g) Western blot results of Runx2, Sox9, Col X, Col II, ALP, and aggrecan protein levels in chondrocytes after mechanical compression at 400 kPa, with addition of DMSO or WZB117. h) Haemotoxylin and eosin (H&E) staining of mandibular condyles in four-week control, four-week FMR, and four-week FMR administered with WZB117 groups. Yellow dashed lines mark the upper proliferative zone and lower hypertrophic zone in cartilage. N = 3 rat/group. Scale bar: 50 μm. i) Graph showing the hypertrophic zone height in four-week control, four-week FMR, and four-week FMR administered with WZB117 groups. j) Graph showing the proliferative zone height in four-week control, four-week FMR, and four-week FMR administered with WZB117 groups. k) Graph showing the average chondrocyte size in four-week control, four-week FMR, and four-week FMR administered with WZB117 groups. *p < 0.05, **p < 0.01, one-way analysis of variance. GAPDH, glyceraldehyde-3-phosphate dehydrogenase; N. S., not significant.

such as ageing, genetics, and systemic disease.[12] Based on this clinical observation, various TMJ degeneration animal models were constructed by disrupting the occlusal states and generating mechanical overloading microenvironments in TMJ. In this study, rat TMJ degeneration was induced by FMR, which was demonstrated to cause anterior disc displacement and abnormal compressive stress on condyle cartilage.[13,14]

Hypertrophic differentiation of chondrocytes is an important pathological change in degenerated cartilage.[15] In addition, hypertrophic chondrocytes also secrete extracellular matrix proteins that lead to the calcification of cartilage, and endothelial growth factors that promote the process of angiogenesis, all of which could accelerate progression of OA. As the sole cell type in cartilage, the homeostasis of chondrocytes, including apoptosis, differentiation, metabolism, and the inflammatory milieu surrounding chondrocytes, are all vital factors influencing OA development.[16-21] In addition, abnormal chondrocyte hypertrophy is a potential therapeutic target for treatment of OA.[22,23] In accordance with this, our study showed that chondrocyte hypertrophy was significantly promoted in FMR-treated rat models. In contrast, the proliferative zone in condyle cartilage was inversely correlated with the hypertrophic zone of cartilage during FMR. Moreover, the hypertrophic transition of chondrocytes was also induced by mechanical compression in vitro, as indicated by increased expressions of Runx2, Col X, and ALP, as well as decreased expressions of Sox9, Col II, and aggrecan. Collectively, both in vivo and in vitro data supported the role of mechanical compression in mediating hypertrophic differentiation of chondrocytes. Regarding the influences of compressive magnitude on chondrocyte hypertrophy, we concluded from the in vitro data that higher magnitude of compression was more efficient in prompting hypertrophy than lower magnitude of compression. Interestingly, the effect of compressions with different magnitudes on chondrogenesis of primary chondrocytes was complex: it seemed that lower compression was beneficial for chondrogenesis compared with uncompressed condition, whereas chondrogenesis was gradually inhibited with increased loading magnitude. This is consistent with previous studies that reported chondrogenetic or hypertrophic differentiation under mechanical stimuli with various types (compressive or stretching), magnitudes (ranging from kPa to MPa), and loading times.[24-27] However, to our knowledge, there are no studies reporting on the mechanisms underlying mechanical stimuli-induced hypertrophic differentiation of chondrocytes.

O-GlcNAcylation has been known as a key regulator of cellular function, by post-translational modification of thousands of proteins, such as chromatin-associated proteins, transcription factors, proteasomal proteins, cytoskeletal proteins, and metabolic enzymes. Tardio et al[28] first found that the pan-O-GlcNAcylation level was significantly increased in the cartilage of human knee with OA, associated with dysregulated expressions of OGT and OGA. Moreover, in vitro stimulation with IL-1β also dramatically elevated O-GlcNAcylation in chondrocytes, suggesting that the proinflammatory milieu in OA cartilage could encourage the accumulation of O-GlcNAcylated proteins in chondrocytes.[28] Furthermore, a recently published study investigated the detailed correlations between O-GlcNAcylation and cartilage degeneration during OA progression – for example, heat-shock transcription

factor 1 (HSF1) facilitated IL-1β-induced OA by increasing O-GlcNAcylation of Notch1, which stabilized Notch1 protein and increased its expression.[29] Another study reported that silencing OGT mitigated lipopolysaccharide (LPS)-induced OA by blocking the binding of NEK7 with NlRP3, which was accomplished via O-GlcNAcylation of NEK7 at Ser204 site, preventing NEK7 phosphorylation. The interaction between NEK7 and NlRP3 incurred chondrocyte pyroptosis, and finally led to OA progression.[30] In addition to these studies reporting O-GlcNAcylation in cartilage, the O-GlcNAcylation in synovium of joint has also been shown to be related to OA, as O-GlcNAc modification was involved in the downregulation of proinflammatory factors TNF-α and IL-8 in synovial cells.[31] Our data showed that during FMR-induced TMJ degeneration, the O-GlcNAcylation level in condyle cartilage was significantly elevated, especially in the deeper layer of cartilage where most hypertrophic chondrocytes reside. This implied the potential role of O-GlcNAcylation in mediating hypertrophic differentiation of chondrocytes during FMR. In order to further confirm this hypothesis, the inhibitor of O-GlcNAcylation, OSMl-1, was applied in both in vivo FMR animals and in vitro compressed chondrocytes. The immunohistochemical and immunoblotting results showed that hypertrophic marker Col X was clearly downregulated by OSMl-1, whereas H&E staining results displayed that hypertrophic differentiation was partially prohibited by OSMl-1. Thus, our study provides strong evidence that FMR- or compression-induced O-GlcNAcylation in chondrocytes is involved in promoting chondrocyte hypertrophic differentiation.

Runx2 has been demonstrated to be a critical mediator of various signals, such as bone morphogenetic protein (BMP), Wnt, and transforming growth factor beta (TGF-β), in promoting chondrocyte hypertrophy and endochondral ossification.[32,33] To date, post-translational modification of Runx2, such as phosphorylation, acetylation, and ubiquitination, has been demonstrated to modulate Runx2 protein activity. Sun et al[34] provided evidence that Runx2 protein could be O-GlcNAc modified in response to high glucose condition using co-immunoprecipitation. Our study extended this finding by illustrating that Runx2 was also O-GlcNAc modified in chondrocytes in a mechanical compression environment. O-GlcNAcylation of Runx2 was shown to increase the binding ability of Runx2 with osteocalcin promoter, thus favouring osteogenic differentiation.[35] Furthermore, O-GlcNAcylation sites in human Runx2 protein were identified, such as Ser32, Ser33, and Ser371, the mutants of which disabled O-GlcNAcylation and pro-osteogenic activity of Runx2.[36,37] However, another study provided contrasting evidence that O-GlcNAcylation of Runx2 resulted in decreased transcriptional activity.[38] We theorized that the discrepancy among these studies was mostly attributed to different cell types, which were mesenchymal cells (C3H10T1/2 cells and bone marrow stem cells) and myogenic C2C12 cells. When chondrocytes were compressed in vitro, we obtained similar results with those studies using mesenchymal cells that O-GlcNAcylation of Runx2 contributed to elevation of its transcriptional activity. Interestingly, although compression induced both Runx2 expression and transcriptional activity, O-GlcNAcylation was only involved in the latter, whereas it had no effect on the former. This was inconsistent with some studies that demonstrated cellular

Mechanical compression induces chondrocyte hypertrophy by regulating Runx2 O-GlcNAcylation during TMJ condyle degeneration
Y. Xiao, Z. Yue, H. Zijing, et al

219

pan-O-GlcNAcylation level influenced the expression of Runx2 in other cells, such as osteogenic cell line MC3T3-E1 and vascular smooth muscle cells.[39,40] Thus, O-GlcNAcylation exerts distinct roles in regulating Runx2 expression and activity in different cell lines. In addition to Runx2, we found that Sox9 protein could also be O-GlcNAc modified in compressed chondrocytes, but the role of O-GlcNAcylation on Sox9 protein remains illusive, since the addition of neither Thiamet G nor OSMI-1 affected Sox9 protein level and activity.

Finally, the mechanism of mechanical compression or FMR-induced hyper-O-GlcNAcylation in chondrocytes was also investigated in this study. Around 2% to 5% of the glucose is metabolized to UDP-GlcNAc through the hexosamine biosynthesis pathway, which is the precursor of O-GlcNAcylation.[41] Thus, the status of O-GlcNAcylation is clearly influenced by intracellular glucose uptake. GLUTs are the major mediators that transport glucose into cells. Studies have shown that manipulations of GLUT function are linked with alterations of protein O-GlcNAcylation.[42,43] Furthermore, O-GlcNAcylation was able to promote GLUT3 expression in endometrial cells, thus creating a positive feedback loop between O-GlcNAcylation and GLUT expression.[44] In the background of cartilage degeneration, it was demonstrated that impaired ability of degenerated chondrocytes to downregulate GLUT1 expression in response to high glucose condition was partially related to ROS overproduction and chondrocyte damage.[11] Inflammatory factors such as IL-8 were shown to upregulate GLUTs expressions, which might be the cause of GLUT overexpression and hyper-O-GlcNAcylation in cartilage degeneration.[45] In our animal model, the GLUT1 level in chondrocytes was significantly elevated compared to that in normal chondrocytes, which correlated well with the condition of O-GlcNAcylation levels. In addition, inhibition of GLUT1 with WZB117 blocked the increased O-GlcNAcylation levels, demonstrating the indispensible role of GLUT1 in mediating elevated O-GlcNAcylation levels in FMR-induced TMJ degeneration. Moreover, WZB117 also prohibited hypertrophic transition of chondrocytes in FMR-induced TMJ degeneration. These studies established the GLUT1-O-GlcNAcylation axis in promoting chondrocyte hypertrophy. However, another study by Wen et al[46] showed that inhibiting GLUT1 and GLUT3 expression facilitated chondrocyte hypertrophy. We assumed that the discrepancy beween their studies and ours was attributed to the different animal models, which was ACLT-induced knee OA in their study and FMR-induced TMJ degeneration in ours. Thus, site-specific differences in chondrocytes, as well as distinct mechanical microenvironments, might cause opposite functions of GLUTs in regulating chondrocyte hypertrophy.

With regard to in vitro mechanical compression model, GLUT1 mRNA and protein levels were also elevated in response to high magnitudes of compression. This finding was consistent with some previous studies that manifested the positive effect of mechanical loading on GLUT1 expression in various other cell types, such as periodontal ligament cells, myotubes, and osteoblasts.[47-50] In addition, inhibition of GLUT1 by WZB117 partially blocked compression-induced hyper-O-GlcNAcylation in chondrocytes, which was consistent with our FMR-induced TMJ degeneration model. Interestingly, the effect of WZB117 on expressions of chondrogenic markers (Sox9, Col II, and aggrecan) and hypertrophic markers

(Runx2, Col X, and ALP) seemed to be independent of dampened O-GlcNAcylation in chondrocytes. For example, WZB117 partially blocked compression-induced expressions of hypertrophic markers and promoted compression-abolished expressions of chondrogenic markers (Figures 6f and 6g), whereas expression of neither chondrogenic markers nor hypertrophic marker Runx2 was affected by O-GlcNAcylation activator Thiamet G and inhibitor OSMI-1 (Figures 5e, 5g, and 5h). Only expressions of hypertrophic markers Col X and ALP were suppressed by both WZB117 and OSMI-1. Therefore, these in vitro data support the fact that compression induces chondrocyte hypertrophic differentiation via increased GLUT1 level; GLUT1 regulates chondrocyte hypertrophy both through the elevation of pan-O-GlcNAcylation that promotes Runx2 activity, and through other unknown pathways that directly affect expression of chondrogenic markers and hypertrophic markers.

In conclusion, this study uncovered a novel mechanism underlying chondrocyte hypertrophy during FMR-induced TMJ degeneration. A compressive microenvironment generated by FMR incurred elevated GLUT1 expression and subsequently promoted intracellular protein O-GlcNAcylation modification. The O-GlcNAcylation of Runx2 regulates its activity, which plays a role in facilitating downstream hypertrophic marker expressions. In addition, elevated GLUT1 might inhibit chondrogenic differentiation and strengthen hypertrophic differentiation via O-GlcNAcylation-independent pathways. These findings highlight the critical involvement of compression, GLUT1, and O-GlcNAcylation in chondrocyte hypertrophic transition, and may also shed light on therapies of FMR-induced progression of TMJ degeneration.

References

1. **Li B**, **Guan G**, **Mei L**, **Jiao K**, **Li H**. Pathological mechanism of chondrocytes and the surrounding environment during osteoarthritis of temporomandibular joint. *J Cell Mol Med*. 2021;25(11):4902–4911.

2. **Rim YA**, **Nam Y**, **Ju JH**. The role of chondrocyte hypertrophy and senescence in osteoarthritis initiation and progression. *Int J Mol Sci*. 2020;21(7):2358.

3. **van der Kraan PM**, **van den Berg WB**. Chondrocyte hypertrophy and osteoarthritis: role in initiation and progression of cartilage degeneration? *Osteoarthritis Cartilage*. 2012;20(3):223–232.

4. **Chatham JC**, **Zhang J**, **Wende AR**. Role of o-linked N-acetylglucosamine protein modification in cellular (patho)physiology. *Physiol Rev*. 2021;101(2):427–493.

5. **Martinez MR**, **Dias TB**, **Natov PS**, **Zachara NE**. Stress-induced O-GlcNAcylation: an adaptive process of injured cells. *Biochem Soc Trans*. 2017;45(1):237–249.

6. **Andrés-Bergós J**, **Tardio L**, **Larranaga-Vera A**, **Gómez R**, **Herrero-Beaumont G**, **Largo R**. The increase in O-linked N-acetylglucosamine protein modification stimulates chondrogenic differentiation both in vitro and in vivo. *J Biol Chem*. 2012;287(40):33615–33628.

7. **Frank D**, **Cser A**, **Kolarovszki B**, **Farkas N**, **Miseta A**, **Nagy T**. Mechanical stress alters protein O-GlcNAc in human periodontal ligament cells. *J Cell Mol Med*. 2019;23(9):6251–6259.

8. **Gerwin N**, **Bendele AM**, **Glasson S**, **Carlson CS**. The OARSI histopathology initiative – recommendations for histological assessments of osteoarthritis in the rat. *Osteoarthritis Cartilage*. 2010;18:S24–S34.

9. **Zheng C**, **Shu J**, **Shao B**, **Liu Z**. Temporomandibular joint stress analysis of patients with different mandibular deformities during unilateral molar occlusion. *Comput Methods Biomech Biomed Engin*. 2024;1–8.

10. **Sun C**, **Shang J**, **Yao Y**, **et al**. O-GlcNAcylation: a bridge between glucose and cell differentiation. *J Cell Mol Med*. 2016;20(5):769–781.

11. **Rosa SC**, **Gonçalves J**, **Judas F**, **Mobasheri A**, **Lopes C**, **Mendes AF**. Impaired glucose transporter-1 degradation and increased glucose transport and oxidative stress in response to high glucose in chondrocytes from osteoarthritic versus normal human cartilage. *Arthritis Res Ther*. 2009;11(3):R80.

12. **Schmitter M**, **Essig M**, **Seneadza V**, **Balke Z**, **Schröder J**, **Rammelsberg P**. Prevalence of clinical and radiographic signs of osteoarthrosis of the temporomandibular joint in an older persons community. *Dentomaxillofac Radiol*. 2010;39(4):231–234.

13. **Pérez del Palomar A**, **Doblaré M**. An accurate simulation model of anteriorly displaced TMJ discs with and without reduction. *Med Eng Phys*. 2007;29(2):216–226.

14. **Teramoto M**, **Kaneko S**, **Shibata S**, **Yanagishita M**, **Soma K**. Effect of compressive forces on extracellular matrix in rat mandibular condylar cartilage. *J Bone Miner Metab*. 2003;21(5):276–286.

15. **Lian C**, **Wang X**, **Qiu X**, **et al**. Collagen type II suppresses articular chondrocyte hypertrophy and osteoarthritis progression by promoting integrin β1-SMAD1 interaction. *Bone Res*. 2019;7:8.

16. **Xu J**, **Ruan Z**, **Guo Z**, **et al**. Inhibition of SAT1 alleviates chondrocyte inflammation and ferroptosis by repressing ALOX15 expression and activating the Nrf2 pathway. *Bone Joint Res*. 2024;13(3):110–123.

17. **Chen M-F**, **Hu C-C**, **Hsu Y-H**, **et al**. The role of EDIL3 in maintaining cartilage extracellular matrix and inhibiting osteoarthritis development. *Bone Joint Res*. 2023;12(12):734–746.

18. **Wang Y**, **Wu Z**, **Yan G**, **et al**. The CREB1 inhibitor 666-15 maintains cartilage homeostasis and mitigates osteoarthritis progression. *Bone Joint Res*. 2024;13(1):4–18.

19. **Lu Y-C**, **Ho T-C**, **Huang C-H**, **Yeh S-I**, **Chen S-L**, **Tsao Y-P**. PEDF peptide plus hyaluronic acid stimulates cartilage regeneration in osteoarthritis via STAT3-mediated chondrogenesis. *Bone Joint Res*. 2024;13(4):137–148.

20. **Mo H**, **Wang Z**, **He Z**, **et al**. Decreased Peli1 expression attenuates osteoarthritis by protecting chondrocytes and inhibiting M1-polarization of macrophages. *Bone Joint Res*. 2023;12(2):121–132.

21. **Piñeiro-Ramil M**, **Sanjurjo-Rodríguez C**, **Rodríguez-Fernández S**, **et al**. Generation of human immortalized chondrocytes from osteoarthritic and healthy cartilage: a new tool for cartilage pathophysiology studies. *Bone Joint Res*. 2023;12(1):46–57.

22. **Kirsch T**, **Swoboda B**, **Nah H-D**. Activation of annexin II and V expression, terminal differentiation, mineralization and apoptosis in human osteoarthritic cartilage. *Osteoarthritis Cartilage*. 2000;8(4):294–302.

23. **Tchetina EV**, **Kobayashi M**, **Yasuda T**, **Meijers T**, **Pidoux I**, **Poole AR**. Chondrocyte hypertrophy can be induced by a cryptic sequence of type II collagen and is accompanied by the induction of MMP-13 and collagenase activity: implications for development and arthritis. *Matrix Biol*. 2007;26(4):247–258.

24. **Juhász T**, **Szentléleky E**, **Somogyi CS**, **et al**. Pituitary adenylate cyclase activating polypeptide (PACAP) pathway is induced by mechanical load and reduces the activity of hedgehog signaling in chondrogenic micromass cell cultures. *Int J Mol Sci*. 2015;16(8):17344–17367.

25. **Deren ME**, **Yang X**, **Guan Y**, **Chen Q**. Biological and chemical removal of primary cilia affects mechanical activation of chondrogenesis markers in chondroprogenitors and hypertrophic chondrocytes. *Int J Mol Sci*. 2016;17(2):188.

26. **Li H**, **Huang L**, **Xie Q**, **et al**. Study on the effects of gradient mechanical pressures on the proliferation, apoptosis, chondrogenesis and hypertrophy of mandibular condylar chondrocytes in vitro. *Arch Oral Biol*. 2017;73:186–192.

27. **Ge Y**, **Li Y**, **Wang Z**, **Li L**, **Teng H**, **Jiang Q**. Effects of mechanical compression on chondrogenesis of human synovium-derived mesenchymal stem cells in agarose hydrogel. *Front Bioeng Biotechnol*. 2021;9:697281.

28. **Tardio L**, **Andrés-Bergós J**, **Zachara NE**, **et al**. O-linked N-acetylglucosamine (O-GlcNAc) protein modification is increased in the cartilage of patients with knee osteoarthritis. *Osteoarthritis Cartilage*. 2014;22(2):259–263.

29. **Huang Y**, **Pan W**, **Bao H**, **Sun X**, **Xu C**, **Ma J**. HSF1 increases EOGT-mediated glycosylation of notch1 to promote IL-1β-induced inflammatory injury of chondrocytes. *Cartilage*. -2024;19476035241229211.

30. **He C**, **Wu Q**, **Zeng Z**, **et al**. OGT-induced O-GlcNAcylation of NEK7 protein aggravates osteoarthritis progression by enhancing NEK7/NLRP3 axis. *Autoimmunity*. 2024;57(1):2319202.

31. **Someya A**, **Ikegami T**, **Sakamoto K**, **Nagaoka I**. Glucosamine downregulates the IL-1β-induced expression of proinflammatory cytokine genes in human synovial MH7A Cells by O-GlcNAc modification-dependent and -independent mechanisms. *PLoS One*. 2016;11(10):e0165158.

32. **Dong Y-F**, **Soung DY**, **Schwarz EM**, **O'Keefe RJ**, **Drissi H**. Wnt induction of chondrocyte hypertrophy through the Runx2 transcription factor. *J Cell Physiol*. 2006;208(1):77–86.

33. **Chen Y**, **Mehmood K**, **Chang Y-F**, **Tang Z**, **Li Y**, **Zhang H**. The molecular mechanisms of glycosaminoglycan biosynthesis regulating chondrogenesis and endochondral ossification. *Life Sci*. 2023;335:122243.

34. **Sun C**, **Lan W**, **Li B**, **et al**. Glucose regulates tissue-specific chondroosteogenic differentiation of human cartilage endplate stem cells via O-GlcNAcylation of Sox9 and Runx2. *Stem Cell Res Ther*. 2019;10(1):357.

35. **Kim S-H**, **Kim Y-H**, **Song M**, **et al**. O-GlcNAc modification modulates the expression of osteocalcin via OSE2 and Runx2. *Biochem Biophys Res Commun*. 2007;362(2):325–329.

36. **Nagel AK**, **Ball LE**. O-GlcNAc modification of the runt-related transcription factor 2 (Runx2) links osteogenesis and nutrient metabolism in bone marrow mesenchymal stem cells. *Mol Cell Proteomics*. 2014;13(12):3381–3395.

37. **Zhang Z**, **Huang Z**, **Awad M**, **et al**. O-GlcNAc glycosylation orchestrates fate decision and niche function of bone marrow stromal progenitors. *Elife*. 2023;12:e85464.

38. **Gu H**, **Song M**, **Boonanantanasarn K**, **et al**. Conditions inducing excessive O-GlcNAcylation inhibit BMP2-induced osteogenic differentiation of C2C12 cells. *Int J Mol Sci*. 2018;19(1):202.

39. **Weng Y**, **Wang Z**, **Fukuhara Y**, **et al**. O-GlcNAcylation drives calcium signaling toward osteoblast differentiation: a bioinformatics-oriented study. *Biofactors*. 2021;47(6):992–1015.

40. **Zhang W**, **Sun Y**, **Yang Y**, **Chen Y**. Impaired intracellular calcium homeostasis enhances protein O-GlcNAcylation and promotes vascular calcification and stiffness in diabetes. *Redox Biol*. 2023;63:102720.

41. **Love DC**, **Hanover JA**. The hexosamine signaling pathway: deciphering the "O-GlcNAc code". *Sci STKE*. 2005;2005(312):re13.

42. **Gu J**, **Jin N**, **Ma D**, **et al**. Calpain I activation causes GLUT3 proteolysis and downregulation of O-GlcNAcylation in Alzheimer's disease brain. *J Alzheimers Dis*. 2018;62(4):1737–1746.

43. **Li T**, **Sun W**, **Zhu S**, **et al**. T-2 toxin-mediated β-arrestin-1 O-GlcNAcylation exacerbates glomerular podocyte injury via regulating histone acetylation. *Adv Sci (Weinh)*. 2024;11(7):e2307648.

44. **Zhang H**, **Qi J**, **Pei J**, **et al**. O-GlcNAc modification mediates aquaporin 3 to coordinate endometrial cell glycolysis and affects embryo implantation. *J Adv Res*. 2022;37:119–131.

45. **Shimizu M**, **Tanaka N**. IL-8-induced O-GlcNAc modification via GLUT3 and GFAT regulates cancer stem cell-like properties in colon and lung cancer cells. *Oncogene*. 2019;38(9):1520–1533.

46. **Wen Z-H**, **Sung C-S**, **Lin S-C**, **et al**. Intra-articular lactate dehydrogenase a inhibitor oxamate reduces experimental osteoarthritis and nociception in rats via possible alteration of glycolysis-related protein expression in cartilage tissue. *Int J Mol Sci*. 2023;24(13):13.

47. **Saito T**, **Okada S**, **Shimoda Y**, **et al**. APPL1 promotes glucose uptake in response to mechanical stretch via the PKCζ-non-muscle myosin IIa pathway in C2C12 myotubes. *Cell Signal*. 2016;28(11):1694–1702.

48. **Wang Y**, **Li Q**, **Liu F**, **et al**. Transcriptional activation of glucose transporter 1 in orthodontic tooth movement-associated mechanical response. *Int J Oral Sci*. 2018;10(3):27.

49. **Moon J-S**, **Lee S-Y**, **Kim J-H**, **et al**. Synergistic alveolar bone resorption by diabetic advanced glycation end products and mechanical forces. *J Periodontol*. 2019;90(12):1457–1469.

50. **Somemura S**, **Kumai T**, **Yatabe K**, **et al**. Physiologic mechanical stress directly induces bone formation by activating glucose transporter 1 (Glut 1) in osteoblasts, inducing signaling via NAD+-dependent deacetylase (sirtuin 1) and runt-related transcription factor 2 (runx2). *Int J Mol Sci*. 2021;22(16):16.

Mechanical compression induces chondrocyte hypertrophy by regulating Runx2 O-GlcNAcylation during TMJ condyle degeneration
Y. Xiao, Z. Yue, H. Zijing, et al

221

Author information

Y. Xiao, MD, PhD Student
Z. Yao, MSc, PhD Student
Z. Xuemin, MD, Research Fellow
Z. Qiang, MD, Research Fellow
Y. Xiao, PhD, MD, Head of Department
R. Dapeng, PhD, MD, Head of Department
Department of Orthodontics, The Affiliated Hospital of Qingdao University, Qingdao, China; School of Stomatology, Qingdao University, Qingdao, China; Department of Central Laboratory, The Affiliated Hospital of Qingdao University, Qingdao, China.

Z. Yue, MD, Research Fellow, Department of Orthodontics, Qingdao Municipal Hospital, University of Health and Rehabilitation Sciences, Qingdao, China.

H. Zijing, MD, PhD Student, Department of Orthodontics, The Affiliated Hospital of Qingdao University, Qingdao, China; Department of Central Laboratory, The Affiliated Hospital of Qingdao University, Qingdao, China.

M. Sui, PhD, Head of Department, College of Materials Science and Engineering, Qingdao University, Qingdao, China.

Author contributions

Y. Xiao: Data curation, Formal analysis, Investigation, Methodology.
Z. Yue: Writing – original draft, Data curation, Formal analysis, Investigation, Methodology.
H. Zijing: Data curation, Formal analysis, Software.
Z. Yao: Data curation, Formal analysis, Investigation, Methodology.
M. Sui: Data curation, Formal analysis, Resources, Software.
Z. Xuemin: Data curation, Formal analysis, Resources, Software.
Z. Qiang: Data curation, Formal analysis, Software.
Y. Xiao: Funding acquisition, Conceptualization, Project administration.
R. Dapeng: Funding acquisition, Project administration, Conceptualization, Writing – original draft, Writing – review & editing.